HHS Public Access

Author manuscript

Cancer Cell. Author manuscript; available in PMC 2016 April 13.

Published in final edited form as:

Cancer Cell. 2015 April 13; 27(4): 502–515. doi:10.1016/j.ccell.2015.03.009.

Mutational Cooperativity Linked to Combinatorial Epigenetic Gain of Function in Acute Myeloid Leukemia

Alan H. Shih[1,2], **Yanwen Jiang**[3,12], **Cem Meydan**[3], **Kaitlyn Shank**[2], **Suveg Pandey**[2], **Laura Barreyro**[4], **Ileana Antony-Debre**[4], **Agnes Viale**[5], **Nicholas Socci**[6], **Yongming Sun**[8], **Alexander Robertson**[8], **Magali Cavatore**[5], **Elisa de Stanchina**[7], **Todd Hricik**[2], **Franck Rapaport**[2], **Brittany Woods**[2], **Chen Wei**[2], **Megan Hatlen**[2], **Muhamed Baljevic**[2], **Stephen D. Nimer**[9], **Martin Tallman**[1], **Elisabeth Paietta**[10], **Luisa Cimmino**[11], **Iannis Aifantis**[11], **Ulrich Steidl**[4], **Chris Mason**[3], **Ari Melnick**[12,14], and **Ross L. Levine**[1,2,13]

[1]Leukemia Service, Memorial Sloan Kettering Cancer Center, New York, NY 10065

[2]Human Oncology and Pathogenesis Program, Memorial Sloan Kettering Cancer Center, New York, NY 10065

[3]Institute for Computational Biomedicine and Department of Physiology and Biophysics, Weill Cornell Medical College, New York, NY 10065

[4]Department of Cell Biology and Division of Hematologic Malignancies, Department of Medicine (Oncology), Albert Einstein College of Medicine, New York, NY 10461

[5]Department of Genomics, Memorial Sloan Kettering Cancer Center, New York, NY 10065

[6]Department of Bioinformatics, Memorial Sloan Kettering Cancer Center, New York, NY 10065

[7]Antitumor Assessment Core Facilities, Memorial Sloan Kettering Cancer Center, New York, NY 10065

[8]Life Technologies, South San Francisco, CA 94080

[9]Sylvester Cancer Center, University of Miami, Miami, FL 33136

[10]Department of Oncology, Montefiore Hospital, Bronx, NY 10467

[11]Department of Pathology and Howard Hughes Medical Institute, NYU School of Medicine, New York, NY 10016

[12]Department of Medicine/Hematology-Oncology and Department of Pharmacology, Weill Cornell Medical College, New York, NY 10065

[13,14]Correspondence: Ross L Levine, Memorial Sloan Kettering Cancer Center, 1275 York Ave, Box 20, New York, NY, 10065, leviner@mskcc.org. Ari Melnick, Weill Cornell Medical College, Cornell University, 413 E 69th Street, BB-1462, New York, NY 10021, amm2014@med.cornell.edu.

Accession numbers

RNA sequencing data has been deposited in GEO under accession number GSE57244 and the eRRBS data under GSE57114.

Summary

Specific combinations of Acute Myeloid Leukemia (AML) disease alleles, including *FLT3* and *TET2* mutations, confer distinct biologic features and adverse outcome. We generated mice with mutations in *Tet2* and *Flt3*, which resulted in fully penetrant, lethal AML. Multipotent *Tet2*$^{-/-}$;*Flt3*^{ITD} progenitors (LSK CD48^{+}CD150^{-}) propagate disease in secondary recipients and were refractory to standard AML chemotherapy and FLT3-targeted therapy. *Flt3*^{ITD} mutations and *Tet2* loss cooperatively remodeled DNA methylation and gene expression to an extent not seen with either mutant allele alone, including at the *Gata2* locus. Re-expression of *Gata2* induced differentiation in AML stem cells and attenuated leukemogenesis. *TET2* and *FLT3* mutations cooperatively induce AML, with a defined leukemia stem cell population characterized by site-specific changes in DNA methylation and gene expression.

Graphical abstract

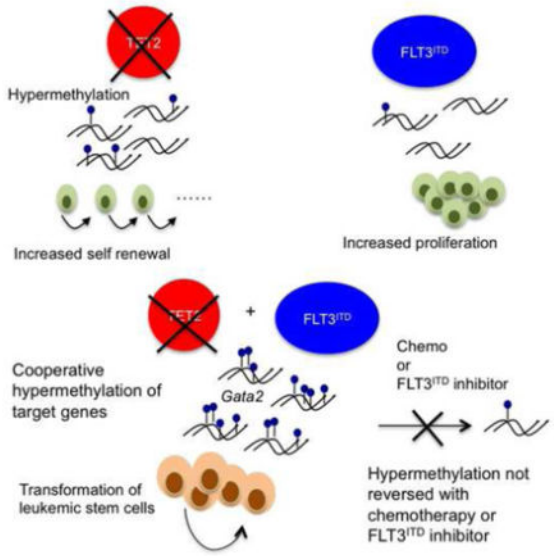

Keywords

Epigenetics; AML; TET2; FLT3

Introduction

Acute Myeloid Leukemia (AML) is the most common acute leukemia in adults; unfortunately, most patients relapse and develop resistance to anti-leukemic therapies. Next-generation sequencing has been used to characterize the AML genome and to identify somatic disease alleles (CGARN, 2013; Welch et al., 2012). Analysis carried out in large AML cohorts have shown that these disease alleles and their combination can be used to improved prognostic schema (Hou et al., 2014; Patel et al., 2012). Recent studies have also demonstrated the biologic and clinical relevance of these alleles, including *TET2*, a gene

targeted by mutations in 10–20% of AML patients (Abdel-Wahab et al., 2009; Delhommeau et al., 2009; Langemeijer et al., 2009).

TET2 mutations are associated with reduced response of AML to chemotherapy and adverse overall survival (Metzeler et al., 2011). In particular, *TET2* mutations are associated with adverse outcome in the setting of concurrent $FLT3^{ITD}$ mutations (Hou et al., 2014; Patel et al., 2012), suggesting these mutations cooperate to induce a poor-prognosis subtype. Mutations in *TET2* lead to loss of function and are often present as heterozygous mutations, although a subset of patients have bi-allelic *TET2* loss (CGARN, 2013; Langemeijer et al., 2009). TET2 catalyzes the 5-hydroxylation of methylcytosine to 5-hydroxymethylcytosine (5-hmC) leading to DNA demethylation (Guo et al., 2011; Tahiliani et al., 2009). *TET2* mutant AML is characterized by reduced 5-hmC levels, increased DNA methylation, and epigenetic silencing (Figueroa et al., 2010; Ko et al., 2010; Rampal et al., 2014). In addition, mutations in *IDH1* and *IDH2* inhibit TET2 function through production of 2-hydroxyglutarate (Figueroa et al., 2010), and *WT1* mutations lead to reduced TET2 function and reductions in 5-hmC (Rampal et al., 2014). Collectively, the TET2 hydroxymethylation pathway is altered by somatic mutations in 25–35% of AML and also in other hematologic and epithelial malignancies.

TET2 regulates hematopoietic stem cell self-renewal. In mouse models, conditional loss of *Tet2* in the hematopoietic compartment leads to expansion of stem cells (LSK, $lin^{-}Sca^{+}cKit^{+}$) and increased repopulation ability in competitive transplantation (Li et al., 2011; Moran-Crusio et al., 2011; Quivoron et al., 2011). *Tet2* mutant mice develop a chronic myeloproliferative disease that does not consistently progress to AML. In the human context, acquired mutations in *TET2* and in genes encoding other epigenetic modifiers (e.g. *DNMT3A*, *ASXL1*) are observed in subjects with clonal hematopoiesis without evidence of an overt hematologic malignancy (Busque et al., 2012; Xie et al., 2014). Analysis of AML and normal subjects suggests mutations in *TET2* and in epigenetic regulators can represent early acquired mutations in “pre-leukemic” stem cells which subsequently acquire further mutations leading to overt transformation (Genovese et al., 2014; Jaiswal et al., 2014; Jan et al., 2012). These data indicate that *TET2* inactivation can contribute to leukemia initiation but is not sufficient to induce transformation to AML.

$Flt3^{ITD}$ mutations are found in nearly 30% of AML and commonly co-occur with *IDH1*, *IDH2*, and *TET2* mutations (Patel et al., 2012). The co-occurrence of $FLT3^{ITD}$ and *TET2* mutations implies these two alleles likely function together to induce transformation. Previous studies have suggested that AML disease alleles cooperate by altering distinct biological mechanisms, classified broadly as those acting on proliferation or on hematopoietic differentiation (Gilliland and Griffin, 2002). However, there are additional possibilities, including the potential for specific combinations of disease alleles to coordinately dysregulate the expression of target loci. This can occur through gain-of-function effects resulting in distinct epigenetic states with a correspondingly altered transcriptional output. Here we investigate loss of *Tet2* together with $Flt3^{ITD}$ in AML development and specifically how they interact to affect transcriptional and epigenetic changes.

Results

Tet2 loss or haploinsufficiency combined with *Flt3^{ITD}* results in AML in vivo

To determine the functional significance of *TET2* and *FLT3^{ITD}* mutations in AML, we generated mice harboring both mutations. Conditional *Vav-cre^{+}Tet2$^{fl/fl}$* (*VTet2$^{-/-}$*) mice were crossed to the constitutive knock-in *Flt3^{ITD}* murine model (Lee et al., 2005) to generate *Vav-cre^{+}Tet2$^{fl/fl}$;Flt3^{ITD}* (*VTet2$^{-/-}$Flt3^{ITD}*) mice. *VTet2$^{-/-}$Flt3^{ITD}* mice were viable at birth with no gross abnormalities; however, all mice expressing both disease alleles developed a lethal hematopoietic disease with a median survival of 36.7 weeks (Figure 1A). The survival of *VTet2$^{-/-}$Flt3^{ITD}* mice was significantly reduced compare to mice expressing either disease allele alone (*VTet2$^{-/-}$*, *Flt3^{ITD}* median survival >80 weeks, p<.0001). After more than one year median follow-up, no *Flt3^{ITD}* mice developed leukemia and less than 30% of *VTet2$^{-/-}$* mice died, due to progressive myeloproliferative neoplasms (MPNs) and not AML. In addition, mice with *Tet2* haploinsufficiency and *Flt3^{ITD}* developed a similar phenotype as *VTet2$^{-/-}$Flt3^{ITD}* mice with median survival of 51 weeks (Figure 1A). We performed further analysis at 4 months when *VTet2$^{-/-}$Flt3^{ITD}* mice had evidence of leukemia. *VTet2$^{-/-}$Flt3^{ITD}* mice showed marked leukocytosis with a median white count of 35.8 k/μl (Figure 1B and S1A). At the time of sacrifice for advanced disease, they developed progressive anemia (median Hct 33.6%, p<.05) which was not observed in mice expressing either disease allele alone (median Hct 40%–51%) (Figure 1C). Analysis of the peripheral blood revealed increased Mac1^{+} cells consistent with myeloid expansion, as well as an expanded cKit^{+} population, and on peripheral smear leukocytes exhibited blast-like morphology with enlarged, open nuclei (Figure 1D, 1E, & S1B).

VTet2$^{-/-}$Flt3^{ITD} mice were characterized by marked splenomegaly (mean 483 mg, p<.05; *Tet2$^{-/-}$* 145 mg, *Flt3^{ITD}* 167 mg, WT 86 mg) and hepatomegaly (Figure 1F & S1C). We observed infiltration of the bone marrow by a monomorphic leukemic population with a decrease in the fraction of mature hematopoietic (lineage^{+}) cells and, by morphology, the number of megakaryocytes (Figure 1G & S1D). There was complete loss of splenic architecture, including germinal centers along with splenic myeloid expansion (Figure 1G & S1E). Similar findings were observed in the lung and liver, with infiltration of leukemic cells in the alveolar and periportal regions (Figure 1G). There was loss of CD71^{+}Ter119^{+} erythroid progenitors in the bone marrow consistent with impaired erythroid differentiation (Figure 1H & S1F). As previously reported for *Flt3^{ITD}* induced disease, phospho-STAT5 levels are elevated in *VTet2$^{-/-}$Flt3^{ITD}* cells compared to wild-type (Figure S1G). To test whether *VTet2$^{-/-}$Flt3^{ITD}* bone marrow cells had a transformed phenotype in vitro, we performed methylcellulose re-plating. Wild-type and *Flt3^{ITD}* cells did not re-plate after three rounds, but *Tet2$^{-/-}$* and *Tet2$^{-/-}$;Flt3^{ITD}* cells both continued to form colonies for 5 rounds of plating, demonstrating *Tet2* loss increases in vitro self-renewal potential in the presence and absence of *Flt3^{ITD}* (Figure 1I). We also performed whole exome sequencing on three *VTet2$^{-/-}$Flt3^{ITD}* leukemias but did not identify any recurrent mutations in leukemia disease alleles (Figure S1H). These data indicate that *Tet2* loss combined with *Flt3^{ITD}* is sufficient to induce AML in vivo.

Tet2 loss and *Flt3^{ITD}* expression results in altered hematopoietic differentiation

Given the known role of *Tet2* in regulating stem cell differentiation, we analyzed stem and progenitor compartments in *VTet2$^{-/-}$Flt3^{ITD}* mice at 4 months. *VTet2$^{-/-}$Flt3^{ITD}* mice had a significantly higher percentage of Granulocyte-Macrophage Progenitors (GMPs, lin$^-$cKit$^+$Sca-1$^-$FcγR$^+$CD34$^+$) (mean, % of lin$^-$ 80%, p<.0001) compared to wild-type (27%) or *VTet2$^{-/-}$* mice (32%), while *Flt3^{ITD}* mice also had an increased GMPs (63%) (Figure 2A & S2A). We observed a significant increase in the absolute number of GMPs in *VTet2$^{-/-}$Flt3^{ITD}* mice compared to wild-type or *VTet2$^{-/-}$* mice (Figure 2B). The increase in the frequency of GMPs was associated with a decrease in the Common Myeloid Progenitor (CMP, lin$^-$cKit$^+$Sca-1$^-$FcγR$^-$CD34$^+$) and Mega-Erythroid Progenitor (MEP, lin$^-$cKit$^+$Sca-1$^-$FcγR$^-$CD34$^-$) populations. The frequency of LSKs was not increased in *VTet2$^{-/-}$Flt3^{ITD}* mice within the lineage$^-$ fraction (Figure 2C); however, we noted a significant expansion in the absolute number of LSK cells (mean, 4.1×10^5 LSKs/mouse vs 0.74×10^5 WT, 1.8×10^5 *VTet2$^{-/-}$*, 2.1×10^5 *Flt3^{ITD}*, p<.05) due to marked expansion of the lineage$^-$ population (Figure 2D & S1D). These data demonstrate that the combination of *Tet2* loss and *Flt3^{ITD}* expression results in synergistic alterations in stem and progenitor cells not seen with either mutant disease allele alone, with expansion of the LSK and GMP populations.

LSK cells and not GMP cells are leukemia initiating cells in *VTet2$^{-/-}$Flt3^{ITD}* mice

Transplantation studies of human leukemias demonstrated that leukemia initiating capacity is highest in CD34$^+$CD38$^-$ stem cells (Bonnet and Dick, 1997). More recent studies have suggested that leukemic stem cell (LSC) activity can also be detected in committed myeloid progenitors (Kirstetter et al., 2008; Sarry et al., 2011). In the murine context, transplantation studies using MLL-fusion leukemia models have shown that GMPs can serve as LSCs, with acquisition of self-renewal by committed progenitors (Heuser et al., 2011; Krivtsov et al., 2006). Since both the LSK and GMP populations are expanded in *VTet2$^{-/-}$Flt3^{ITD}* mice, we sought to determine if either population had leukemia initiating capacity. LSK and GMP cells were sorted from bone marrow of CD45.2 *VTet2$^{-/-}$Flt3^{ITD}* mice and transplanted into CD45.1 recipient mice. Mice transplanted with LSK cells but not GMP cells had progressive expansion of the CD45.2 donor population (Figure 2E & S2B). LSK transplanted mice developed disease similar in phenotype to primary mice, with splenomegaly, expansion of cKit$^+$ blasts, and similar stem and progenitor frequencies in the bone marrow re-establishing the leukemic hierarchy (Figure 2F, 2G, & S2C). These data demonstrate the LSK, but not the GMP, population has leukemic initiating potential.

The LSK population in *VTet2$^{-/-}$Flt3^{ITD}* mice displayed a monomorphic immunophenotype consistent with selective expansion of the multipotent progenitor (MPP) population (LSK CD48$^+$CD150$^-$) (mean % of LSK 91% vs WT 59%, p<.001) (Figure 2H & S2D). By contrast, we observed near-complete loss of the long-term HSCs (LT-HSC) (LSK CD48$^-$CD150$^+$) population (mean % of LSK 0.04% vs WT 8.2%, p<.01) (Figure 2H & S2D–F). The frequencies of these populations were also different from single mutant mice, and maintained in secondarily transplanted mice (Figure S2D and S2E). Secondary transplantation of sorted MPPs resulted in leukemic engraftment similar to that observed with sorted LSKs (Figure S2G and S2H). Thus, the MPP population, which is normally

more limited in self-renewal capacity, acquires self-renewal and LSC potential with *Tet2* and *Flt3* mutations.

The observation that LSKs, but not GMPs, could initiate leukemia in secondary recipients suggested that *Tet2* loss could increase the self-renewal of LSKs but not of more committed myeloid progenitors. Because the acquisition of serial re-plating potential is due to *Tet2* loss and not dependent on $Flt3^{ITD}$, we investigated the impact of *Tet2* loss on LSK and GMP cells in methylcellulose assays (Figure 2I). $Tet2^{-/-}$ LSK cells had serial re-plating potential, whereas $Tet2^{-/-}$ GMP cells did not persist beyond the third plating. This supports the observation that LSK and not GMP derived cells are transformed by loss of *Tet2*, and that the self-renewal program induced by *Tet2* loss is able to transform early stem-progenitors, but not more committed populations. This is in contrast to MLL-fusion driven leukemia, which is capable of transforming GMPs to LSCs in vivo.

We next sought to determine stem and progenitor frequencies in AML patients with concurrent *TET2* and $FLT3^{ITD}$ mutations (n=9). $TET2;FLT3^{ITD}$ mutant AML patients were characterized by a marked expansion in the proportion of ST-HSC/MPPs but variable numbers in the proportion of LT-HSCs and GMPs (Figure 2J, S2I–P). We also observed a significant reduction in the proportion of CMPs (Figure S2K). Mutational analysis of sorted populations (n=6) showed that *TET2* mutations were seen in LT-HSCs, ST-HSCs/MPPs, CMPs and GMPs, suggesting that *TET2* mutations are acquired in hematopoietic stem cells (Figure S2Q). $FLT3^{ITD}$ was also detectable in all these populations; however, they tended to be present at a lower allelic burden than the *TET2* mutation (Figure S2Q). This is in agreement with the model in which *TET2* mutations lead to pre-leukemic clones that with additional mutations progress to AML and expand specific subpopulations (Jan et al., 2012). In addition, these data support the notion that the expansion of ST-HSC/MPPs in $TET2;FLT3^{ITD}$ mutant AML is not due to selective acquisition of these mutations in this compartment but rather due to clonal expansion of specific populations in $TET2;FLT3^{ITD}$ mutant AML.

$VTet2^{-/-}Flt3^{ITD}$ AML is refractory to chemotherapy

In order to assess the impact of anti-leukemic therapies on $VTet2^{-/-}Flt3^{ITD}$ AML cells compared to normal hematopoietic cells, we tested the therapeutic efficacy of doxorubicin and cytarabine in CD45.1 mice transplanted with CD45.2 $VTet2^{-/-}Flt3^{ITD}$ AML cells (n=5 per group). Mice were treated with vehicle or doxorubicin and cytarabine for 5 to 7 days followed by assessment of disease burden (Figure 3A). Induction chemotherapy with doxorubicin and cytarabine induced pancytopenia with a similar severity and kinetic as observed with induction therapy in human AML (Figure S3A). This therapy was effective in reducing and in some cases eliminating the leukemic clone in AML1-ETO driven leukemias, consistent with previous reports (Figure S3B–G) (Zuber et al., 2009). In $VTet2^{-/-}Flt3^{ITD}$ disease, chemotherapy resulted in a transient decrease in the proportion of AML (CD45.2) cells; however by 4 weeks all mice again developed marked leukocytosis (Figure 3B). Furthermore with recovery from pancytopenia, the AML clone had expanded and there was no reduction in splenomegaly (Figure 3C & S3H). Thus, $VTet2^{-/-}Flt3^{ITD}$ AML is chemoresistant relative to other, sensitive AML genotypes.

VTet2$^{-/-}$*Flt3*^{ITD} LSCs are refractory to FLT3-targeted therapy

FLT3 inhibitors have clinical activity in *FLT3*^{ITD} mutant AML but do not achieve sustained remission (Kayser and Levis, 2014; Smith et al., 2012). To understand the nature of this response, we assessed leukemic burden in mice transplanted with *VTet2*$^{-/-}$*Flt3*^{ITD} cells following treatment with the FLT3 inhibitor AC220 (n=5) (Figure 3A). AC220 treatment (10 mg/kg) for 4 weeks led to a reduction in leukocyte count and a modest reduction in spleen weight and leukemic burden (Figure 3B, 3C, & S3H). However, we observed persistent cKit^{+} blast cells in the blood of mice treated with AC220 therapy (Figure 3D). This is in contrast to reported FLT3 inhibition in *Flt3*^{ITD} mice where aberrant differentiation is effectively reversed (Chu et al., 2012).

We next assessed differential effects of FLT3 inhibition on LSCs and on bulk leukemia cells. We treated primary *VTet2*$^{-/-}$*Flt3*^{ITD} mice with vehicle or AC220 (10 mg/kg) (n=3 per group). Mice treated with AC220 for 3 weeks had smaller spleens and reduced WBC counts consistent with an inhibitory effect on the bulk leukemic population (Figure 3E & 3F). AC220 therapy increased the proportion of MEP cells while decreasing that of GMPs, suggesting that myeloid progenitors remain sensitive to FLT3 inhibition (Figure 3G). By contrast, FLT3 inhibition did not reduce the absolute number of LSK cells indicative of a lack of efficacy on AML LSCs (Figure 3H). There was a trend towards increased LSK frequency due to a relative decrease in the other cell populations (Figure 3H). In addition, AC220 therapy did not inhibit LSC function, as recipients transplanted with cells from AC220 treated mice developed disease with similar kinetics as those from vehicle treated mice (Figure S3I and S3J). Furthermore, treatment with induction chemotherapy or with AC220 did not alter the immunophenotype of the LSK compartment, with continued expansion of the MPPs and reduction of the LT-HSCs (Figure 3I). These data indicate that *VTet2*$^{-/-}$*Flt3*^{ITD} LSCs are refractory to FLT3 targeted therapy and to cytotoxic chemotherapy, and suggest that there may be specific gain-of-function gene regulatory effects by combinatorial actions of *Tet2*$^{-/-}$ and *Flt3*^{ITD} in LSCs that confer this phenotype.

Transcriptional and Methylation Profiling Reveal that *VTet2*$^{-/-}$*Flt3*^{ITD} LSC Have a Unique Signature

In order to understand the basis for the leukemic phenotype, we performed RNA sequencing on LSK and GMP cells from wild-type and *VTet2*$^{-/-}$*Flt3*^{ITD} mice. Unsupervised hierarchical clustering showed that LSK cells from wild-type and mutant mice were more similar to each other than to GMPs of the same genotype, again supporting the observation that mutant GMPs had not gained a stem-like signature (Figure 4A & S4A). Compared to wild-type LSK cells, *Tet2*$^{-/-}$;*Flt3*^{ITD} LSKs had a distinct gene expression signature, with dysregulated expression of known self-renewal and differentiation genes including *Id1*, *Gata1*, *Gata2*, *Mpl*, and *Socs2* (Figure 4B, S4B & Table S1, S2). This signature also was distinct from *Tet2*$^{-/-}$ or *Flt3*^{ITD} LSKs (Figure S4C). GSEA analysis showed that *VTet2*$^{-/-}$*Flt3*^{ITD} LSK cells were characterized by enrichment of an embryonic stem cell signature and reduced expression of a *GATA* target signature (Figure 4C) (Liberzon et al., 2011; Wong et al., 2008).

Previous studies have shown that *TET2* mutant AMLs are characterized by site-specific changes in DNA methylation (Akalin et al., 2012a; Figueroa et al., 2010). We therefore performed methylation profiling of *VTet2*$^{-/-}$*Flt3*^{ITD}, single mutant, and wild-type LSK cells using enhanced reduced representation bisulfite sequencing (eRRBS) to evaluate CpG regions (Table S3). Hierarchical clustering by differentially methylated cytosines (DMCs) demonstrated clear separation of leukemic *VTet2*$^{-/-}$*Flt3*^{ITD} LSKs from WT LSKs (Figure 4D). We next analyzed the grouping of DMCs into differentially methylated regions (DMRs). The majority of DMRs in *VTet2*$^{-/-}$*Flt3*^{ITD} LSKs were located in gene regulatory elements, with a distribution that was distinct from those of single mutant LSKs (Figure 4E & S4D). CpG islands and particularly CpG shores have been described to be critical regulatory regions for hematopoiesis (Ji et al., 2010). Hypermethylated DMRs in *VTet2*$^{-/-}$*Flt3*^{ITD} LSKs were more frequently located in promoter regions and CpG shores compared to other DMRs groups, suggesting gene regulatory function (Figure 4E & S4D). Principle component analysis of the differentially methylated regions (DMRs) showed that *VTet2*$^{-/-}$*Flt3*^{ITD} LSK cells form a separate group from single mutants LSKs, suggesting a functional correlation between genotype and variation in methylation (Figure S4E). GSEA analysis demonstrated hypermethylated promoter regions were enriched for genes with a trend in decreased expression based on RNA-seq data, consistent with epigenetic silencing through hypermethylation (Figure 4F). We identified 58 genes with altered differential expression and promoter or gene body hypermethylation in *VTet2*$^{-/-}$*Flt3*^{ITD} LSK cells compared to wild-type (Table S4). These include *Gata2*, *Hox* genes, *Smarca2*, and *Dusp4*, genes with known roles in hematopoiesis and differentiation. These data indicate that key regulatory genes are epigenetically modified and altered in expression as a result of *Tet2* and *Flt3* mutation.

Concurrent *Tet2* and *Flt3*^{ITD} mutations result in synergistic effects on DNA methylation and gene expression

With the observation that concurrent mutations in *Tet2* and *Flt3*^{ITD} cooperate to induce AML, we hypothesized that the combination of these disease alleles would result in a synergistic effect on the epigenetic state and on gene expression. Compared to *Tet2*$^{-/-}$ or *Flt3*^{ITD} LSKs, *Tet2*$^{-/-}$;*Flt3*^{ITD} LSKs had a dramatic increase in the number of DMRs; we observed 1704 DMRs in *Tet2*$^{-/-}$;*Flt3*^{ITD}, 174 in *Tet2*$^{-/-}$, and 200 in *Flt3*^{ITD} LSKs (Figure 5A). *Tet2*$^{-/-}$ LSKs displayed proportionally greater hypermethylation versus wild-type LSKs, whereas *Flt3*^{ITD} LSKs had predominant hypomethylation. The combination of *VTet2*$^{-/-}$*Flt3*^{ITD} had greater DNA hypermethylation, similar in direction (but not in extent) to that observed in *Tet2*$^{-/-}$ LSK cells (Figure 5B). We observed that *Tet2*$^{-/-}$;*Flt3*^{ITD} mutation resulted in DMCs at loci distinct from those affected in *Flt3*^{ITD} or *Tet2*$^{-/-}$ LSKs (Figure S5A); similarly, the number of hypermethylated DMCs per genetic loci was also significantly different (Figure 5C). The majority of genes with DMRs in *Tet2*$^{-/-}$;*Flt3*^{ITD} LSKs were unique from the smaller set of those observed in *Tet2*$^{-/-}$ or *Flt3*^{ITD} LSKs (Figure 5D). Therefore, the impact of *Tet2*$^{-/-}$;*Flt3*^{ITD} mutations on DNA methylation was much greater than would be expected from the additive effects of single *Tet2* and *Flt3*^{ITD} mutations, implying changes in methylation are a consequence of the cooperative effects of *Tet2* loss and *Flt3*^{ITD}.

In order to identify target loci with potential functional relevance, we focused on genes with altered expression and methylation in the setting of concurrent *Tet2* and *Flt3*^{ITD} mutations. We identified the set of differentially expressed genes in *VTet2*$^{-/-}$*Flt3*^{ITD}, and then target loci where the combination of *Tet2* and *Flt3*^{ITD} mutations had a cooperative gain-of-function effect on methylation using logistic regression and pairwise comparisons (*VTet2*$^{-/-}$*Flt3*^{ITD} vs single mutants). We identified 115 genes that exhibited cooperative effects on DNA methylation (>=3 DMCs) and altered expression (Tables S5, S6, & Figure S5B). For the majority of the loci that demonstrated cooperativity, we observed DNA hypermethylation and transcriptional silencing (Table 1 & Figure 5E). The pattern of expression of the subset of these genes with the greatest methylation differences (>=6 DMRs, see Table 1), demonstrated a distinct expression profile in *Tet2*$^{-/-}$;*Flt3*^{ITD} LSKs compared to wild-type or single mutant LSKs (Figure 5F). Notably, of the 27 genes with promoter DMRs and differential expression, 19 were differentially methylated in *TET2* mutant AML patients (Table S6) (Akalin et al., 2012a). We next analyzed methylation in ST-HSC cells from *TET2;FLT*^{ITD} AML patients (n=2) by performing eRRBS and compared DNA methylation to normal CD34^{+} cells (n=13). We identified 83 genes which had at least 5 promoter DMCs in murine *Tet2*$^{-/-}$;*Flt3*^{ITD} LSKs compared to wild-type LSKs and also had a human ortholog; 53 of these 83 genes had at least one DMC in *TET2;FLT3*^{ITD} AML ST-HSCs ($p=4.8 \times 10^{-8}$), and 33 of 83 had 5 or more DMCs ($p=2.8 \times 10^{-6}$) (Table S7).

Epigenetic silencing of *Gata2* contributes to impaired differentiation in *VTet2*$^{-/-}$*Flt3*^{ITD} LSC

The *Gata2* locus in *VTet2*$^{-/-}$*Flt3*^{ITD} LSKs was characterized by a marked hypermethylation at the promoter, introns, and a key enhancer region compared to wild-type and single mutant LSKs (Figure 5G) (Snow et al., 2010). Expression analysis of *Gata2* in sorted LSK cells demonstrate that concomitant *Tet2* and *Flt3*^{ITD} mutations led to significant decreased levels of RNA expression (Figure 5H). The *GATA2* locus was also densely hypermethylated in human *TET2; FLT3*^{ITD} AML cells, with 45 DMCs in the *GATA2* locus in leukemic ST-HSCs compared to normal CD34^{+} cells (Figure 5G).

To determine the impact of *Flt3*^{ITD} inhibition on *Gata2* expression, we assessed the expression level of *Gata2* in LSK cells sorted from vehicle or AC220 treated *VTet2*$^{-/-}$*Flt3*^{ITD} mice. *Gata2* expression modestly increased with AC220 therapy, but did not return to wild-type levels (Figure S5C). This suggests that the cooperative activities of both mutations are required to epigenetically silence the *Gata2* locus and that targeting one mutant allele alone is not sufficient to reverse the coordinate effects on the transcriptome. We then analyzed the impact of FLT3 inhibition with AC220 on locus-specific DNA methylation in *VTet2*$^{-/-}$*Flt3*^{ITD} LSKs. Despite evidence of effect on bulk leukemia cells with reductions in WBC count and spleen size, AC220 treatment did not substantively alter the overall LSK methylation status as individual DMRs remained highly correlated between naïve and treated LSKs (Figure 5I and S5D–F). Clustering by methylation status showed that AC220-treated LSKs were indistinguishable from vehicle treated or naïve *VTet2*$^{-/-}$*Flt3*^{ITD} LSKs and were distinct from *Tet2*$^{-/-}$ LSKs (Figure S5G and S5H). Consistent with the transcriptional data, the methylation status of *Gata2* locus was largely unaffected by AC220 therapy (Figure 5G).

We next sought to assess whether restoring *Gata2* expression would alter differentiation and inhibit leukemogenesis in *VTet2*$^{-/-}$*Flt3*^{ITD} cells. We expressed *Gata2* and MIGR1 control using a GFP-expressing vector in bone marrow cells from *VTet2*$^{-/-}$*Flt3*^{ITD} mice. When plated in methylcellulose, control *VTet2*$^{-/-}$*Flt3*^{ITD} colony cells showed reduced CD71 positivity, consistent with impaired erythroid differentiation (Figure 5J & S5I). By contrast, *VTet2*$^{-/-}$*Flt3*^{ITD} cells re-expressing *Gata2* had increased CD71 expression (Figure 5J & S5I). These data imply *Tet2*$^{-/-}$; *Flt3*^{ITD} bone marrow cells are not irrevocably blocked but are capable of differentiating when *Gata2* is re-expressed. We next assess the impact of re-expressing *Gata2* in vivo by transplanting *Tet2*$^{-/-}$;*Flt3*^{ITD} bone marrow cells expressing control GFP or *Gata2* into recipient mice. Cells expressing *Gata2* engrafted in vivo; however, we observed a marked reduction in the proportion of *Gata2* positive *VTet2*$^{-/-}$*Flt3*^{ITD} myeloid leukemia cells compared to *Gata2* positive erythroid cells, consistent with in vivo erythroid differentiation of AML cells (Figure 5K). Furthermore, *Gata2* expression, but not expression of vector control, resulted in a progressive reduction in the proportion of cKit^{+} *Tet2*$^{-/-}$;*Flt3*^{ITD} leukemic cells, correlating with disappearance of the AML clone (Figure 5K & S5J). Notably, mice expressing vector alone succumbed to leukemia, whereas no mice expressing *Gata2* developed lethal AML (Figure 5L). These data demonstrate that *Gata2* re-expression can restore differentiation and attenuates leukemogenesis in vivo.

Discussion

Mutations that dysregulate the DNA hydroxy-methylcytosine pathway are amongst the most common disease alleles in human cancers and include mutations in *TET2*, as well as mutations in *IDH*1, *IDH2*, and *WT1* that can lead to inhibition of TET2 function. As such, there is a need to delineate how these mutations contribute to malignant transformation, the epigenetic state, and alterations in transcriptional output. Here we show that *Tet2* loss combined with *Flt3*^{ITD} causes leukemia in vivo, and that these two disease alleles cooperate to induce synergistic and gain-of-function effects on DNA methylation and gene expression.

Previous studies using *Tet2* conditional knock-out mice implicate a role for TET2 in regulating stem cell self-renewal. These data with studies demonstrating *TET2* mutations establishing clonal hematopoiesis and a pre-leukemic state in the human context, suggest that *TET2* mutations enhance stem cell function and initiate the process of malignant transformation. Similarly, studies have shown that a broader spectrum of leukemia disease alleles, including those in *DNMT3A* and in *ASXL1*, can promote clonal hematopoiesis without inducing AML. *TET2* loss has a second, critical function in leukemic transformation, as it can cooperate with other AML disease alleles to coordinately dysregulate DNA methylation and alter expression at target loci. This effectively maintains the block in hematopoietic differentiation and increases self-renewal of AML LSCs after malignant transformation. These data demonstrate a role for *TET2* mutation in leukemic maintenance distinct from inducing clonal expansion, and suggest that mutations in epigenetic modifiers can act at multiple steps during leukemogenesis.

We identify the LSC population in our model of *TET2;FLT3*^{ITD} mutant AML in the MPP compartment, a population that has also been found to be expanded in human AML samples

and to be capable of leukemia propagation in xenotransplant studies (Goardon et al., 2011). Although the combination of *Tet2* and *Flt3* mutations in our mouse model was sufficient to promote leukemogenesis, additional mutations and chromosomal alterations are sometimes seen in *TET2;FLT3*^{ITD} mutant human AML (CGARN, 2013), suggesting additional events may be required to transform human LSCs. However, we find significant overlap between the set of differentially methylated genes in our model and in human AML stem-progenitor cells suggesting that this combination of mutations leads to similar effects on DNA methylation.

Although the *TET* family of enzymes is critical in regulating DNA methylation, the target genes and pathways affected have not been well characterized in AML or other human cancers. We demonstrate that *Tet2;Flt3*^{ITD} mutant AML has a unique epigenetic and transcriptional signature, and that LSCs in *Tet2;Flt3*^{ITD} mutant AML are characterized by increased expression of a stem cell gene expression program and by reduced expression of *Gata2* and of a *GATA*-associated gene expression signature. These data underscore recent studies showing that *Idh2;Flt3*^{ITD} mutant AML is characterized by a reduced *GATA* gene expression signature (Kats et al., 2014) and that *IDH1 and IDH2* mutant AML samples are characterized by differential methylation of *GATA* target genes (Figueroa et al., 2010). Consistent with these data, we found that *GATA2* is hypermethylated in *TET2;Flt3*^{ITD} human AML stem-progenitor cells. Furthermore, AML profiling has identified somatic *GATA2* mutations and dysregulated *GATA2* expression (Celton et al., 2014; CGARN, 2013; Groschel et al., 2014). Our data is also consistent with reports in which human hematopoietic stem cell differentiation to the erythroid lineage acquires 5-hmC at binding sites enriched for GATA1 and GATA2 motifs and depends on TET2 (Madzo et al., 2014; Pronier et al., 2011). Undoubtedly, there are additional genes that are dysregulated in *TET2* and *IDH* mutant AMLs that can contribute to leukemic transformation; they may also vary depending on the specific cooperating mutation.

Although loss of *Tet2* alone leads to alterations in DNA methylation and gene expression, we found that the combination of *Tet2* loss with expression of *FLT3*^{ITD} results in synergistic and gain-of-function effects on the epigenetic state and on transcription. Previous studies in AML and in other malignancies have suggested that different somatic mutations combine to induce transformation by endowing a cancer cell with discrete, necessary biologic features; our data suggest that there may be specific target genes that serve as convergent nodes for cooperative transformation requiring combinations of mutations. We observe that inhibition of FLT3 signaling alone is not sufficient to reverse the methylation changes in *Tet2;Flt3*^{ITD} mutant LSCs. One could speculate that since TET2 is required for demethylation, once certain CpGs become methylated in the combined *TET2;FLT3*^{ITD} mutant setting, even if FLT3 signaling is blocked, without sufficient TET2 activity, the methylation status cannot be reset. This provides another possible mechanism of resistance to FLT3 directed therapy; specifically the persistent altered epigenetic state of LSCs that is not reversed by FLT3 inhibitor monotherapy.

The observation that ectopic expression of *Gata2* can promote differentiation of *VTet2*$^{-/-}$*Flt3*^{ITD} mutant AML cells demonstrates that *Tet2;Flt3*^{ITD} mutant LSCs have an epigenetic signature that does not irrevocably alter their differentiation and self-renewal

potential. These data suggest that therapies that can reverse this signature will offer significant therapeutic efficacy in AML patients with mutations in *TET2*, *IDH1*, or *IDH2*. This may include combination therapies which incorporate epigenetic modulators such as hypomethylating agents and bromodomain inhibitors, or targeted therapies such as the mutant IDH1 and IDH2 inhibitors (Rohle et al., 2013; Wang et al., 2013). Clinical studies indicate increased sensitivity to hypomethylating agents in *TET2* mutant patients (Bejar et al., 2014; Traina et al., 2014), which may reflect an ability to reverse the effects of *TET2* mutations on DNA methylation by these agents. Studies in preclinical models and in the clinical setting will determine if these or other epigenetic therapies can be used to potently and specifically reprogram leukemia stem cells to induce differentiation, and to determine how best to incorporate epigenetically targeted agents into multimodality therapies.

Experimental Procedures

Transgenic Animals

The conditional *Vav-cre*$^{+}$ *Tet2*$^{fl/fl}$ mice were previously described (Moran-Crusio et al., 2011) and *Flt3*^{ITD} mice were kindly provided by Gary Gilliland (University of Pennsylvania). Pathology was obtained after fixation in 4% PFA and slides stained with H&E. All animal procedures were conducted in accordance with the Guidelines for the Care and Use of Laboratory Animals and were approved by the Institutional Animal Care and Use Committees at MSKCC.

In vitro colony forming assays

Bone marrow cells (whole or sorted populations) were seeded into cytokine supplemented methylcellulose medium (Methocult, M3434, Stem Cell Technologies). Colonies propagated in culture were scored at day 7 to 10. Cells were resuspended and re-plated at 15,000 cells per well.

Bone marrow transplantation

Dissected femurs and tibias were isolated. Bone marrow was flushed with a syringe into RPMI 10%FCS media. Spleens were isolated and single cell suspensions made by mechanical disruption using glass slides. Cells were passed through a 70 μm strainer. RBCs were lysed in ammonium chloride-potassium bicarbonate lysis buffer for 10 minutes on ice. Finally, 1×10^6 total cells were transplanted via tail vein injection into lethally irradiated (2x 550 Rad) C57BL/6 or CD45.1 host mice. For sorted cell populations, $1{\times}10^5$ (LSK), $3{\times}10^5$ (GMP), $4{\times}10^5$ (GFP^{+}) cells were transplanted in combination with support marrow.

In vivo treatment studies

Mice were treated daily using oral gavage with AC220 at 10 mg/kg, suspended in 5% 2-hydroxypropyl-β-cyclodextrin. Mice were treated with combination chemotherapy using protocol previously described (Zuber et al., 2009). Briefly, mice were treated for 5 to 7 days daily with i.p. injections of 100 mg/kg cytarabine and 3 days, 3 mg/kg doxorubicin.

RNA sequencing and Analysis

Cell populations were sorted using BD FACSAria and RNA isolated using TrizolLS. RNA was prepared using RiboMinus from LifeTechnologies. The library was sequenced using the Ion Proton System from LifeTechnologies. Aligned RNA was analyzed for fold change. See supplement for details of analysis.

eRRBS and Differential Methylation Analysis

eRRBS was performed using a protocol previously described (Akalin et al., 2012a). Briefly, genomic DNA were digested with MspI. DNA fragments were end-repaired, adenylated and ligated with Illumina kits. Library fragments of 150–250 bp and 250–400 bp were isolated. Bisulfite treatment was performed using the EZ DNA Methylation Kit (Zymo Research). Libraries were amplified and sequenced on an Illumina HiSeq. Differential methylation analysis was performed on the resulting eRRBS data using methylKit (Akalin et al., 2012b) for finding single nucleotide differences (q-value < 0.01 and methylation percentage difference of at least 25%) and eDMR (Li et al., 2013) for finding differentially methylated regions. See supplement for details of analysis.

Retroviral transduction

MSCV *Gata2* construct was provided by Dr. John Crispino (Northwestern). Virus was produced by transfecting 293T cells with MSCV and EcoPack plasmids. Bone marrow was harvested 6 days after 5FU (150 mg/kg) treatment. After red cell lysis, the cells were cultured in media containing RPMI/10% FBS and IL-3 (7 ng/ml), IL-6 (10 ng/ml), and stem cell factor (10 ng/ml). Cells were infected twice in the presence of polybrene and Hepes buffer.

Flow cytometry and FACS

Antibody staining and FACS analysis were performed as previously described (Moran-Crusio et al., 2011). Intra-cytoplasmic staining was performed with the Cytofix Cytoperm kit from BD Biosciences. Stem cell enrichment was performed using the Progenitor Cell Enrichment Kit (Stem Cell Technologies). Isolation of human stem and progenitor populations from mononuclear cells was performed as previously described (Barreyro et al., 2012). See supplement for antibodies.

Patient Samples

AML samples were obtained at diagnosis from patients enrolled in the Eastern Cooperative Oncology Group’s (ECOG) 1900 clinical trial. All patients provided informed consent. Approval was obtained from the Institutional Review Board at Memorial Sloan-Kettering Cancer Center.

Supplementary Material

Refer to Web version on PubMed Central for supplementary material.

Acknowledgments

This work was supported by a Gabrielle's Angel Fund grant to RLL and AMM, a Leukemia Lymphoma Society (LLS) Translational Research grant to RL and IA, grant CA172636-01 to RLL, IA and AM, and the Samuel Waxman Cancer Research Center. CEM is supported by R01HG006798, R01NS076465; SN and MH by R01CA166835; MSKCC cores by P30 CA008748. AM is a Burroughs Wellcome Clinical Translational Scholar and supported by the Sackler Center for Biomedical and Physical Sciences. RLL is a LLS Scholar. AHS is supported by the Conquer Cancer Foundation and LLS. YJ is an ASH Scholar. We would like to thank Scott Lowe for reagents and advice on chemotherapy studies.

References

Abdel-Wahab O, Mullally A, Hedvat C, Garcia-Manero G, Patel J, Wadleigh M, Malinge S, Yao J, Kilpivaara O, Bhat R, et al. Genetic characterization of TET1, TET2, and TET3 alterations in myeloid malignancies. Blood. 2009; 114:144–147. [PubMed: 19420352]

Akalin A, Garrett-Bakelman FE, Kormaksson M, Busuttil J, Zhang L, Khrebtukova I, Milne TA, Huang Y, Biswas D, Hess JL, et al. Base-pair resolution DNA methylation sequencing reveals profoundly divergent epigenetic landscapes in acute myeloid leukemia. PLoS Genet. 2012a; 8:e1002781. [PubMed: 22737091]

Akalin A, Kormaksson M, Li S, Garrett-Bakelman FE, Figueroa ME, Melnick A, Mason CE. methylKit: a comprehensive R package for the analysis of genome-wide DNA methylation profiles. Genome Biol. 2012b; 13:R87. [PubMed: 23034086]

Barreyro L, Will B, Bartholdy B, Zhou L, Todorova TI, Stanley RF, Ben-Neriah S, Montagna C, Parekh S, Pellagatti A, et al. Overexpression of IL-1 receptor accessory protein in stem and progenitor cells and outcome correlation in AML and MDS. Blood. 2012; 120:1290–1298. [PubMed: 22723552]

Bejar R, Lord A, Stevenson K, Bar-Natan M, Perez-Ladaga A, Zaneveld J, Wang H, Caughey B, Stojanov P, Getz G, et al. TET2 mutations predict response to hypomethylating agents in myelodysplastic syndrome patients. Blood. 2014; 124:2705–2712. [PubMed: 25224413]

Bonnet D, Dick JE. Human acute myeloid leukemia is organized as a hierarchy that originates from a primitive hematopoietic cell. Nature medicine. 1997; 3:730–737.

Busque L, Patel JP, Figueroa ME, Vasanthakumar A, Provost S, Hamilou Z, Mollica L, Li J, Viale A, Heguy A, et al. Recurrent somatic TET2 mutations in normal elderly individuals with clonal hematopoiesis. Nat Genet. 2012; 44:1179–1181. [PubMed: 23001125]

Celton M, Forest A, Gosse G, Lemieux S, Hebert J, Sauvageau G, Wilhelm BT. Epigenetic regulation of GATA2 and its impact on normal karyotype acute myeloid leukemia. Leukemia. 2014

CGARN CGARN. Genomic and epigenomic landscapes of adult de novo acute myeloid leukemia. N Engl J Med. 2013; 368:2059–2074. [PubMed: 23634996]

Chu SH, Heiser D, Li L, Kaplan I, Collector M, Huso D, Sharkis SJ, Civin C, Small D. FLT3-ITD knockin impairs hematopoietic stem cell quiescence/homeostasis, leading to myeloproliferative neoplasm. Cell Stem Cell. 2012; 11:346–358. [PubMed: 22958930]

Delhommeau F, Dupont S, Della Valle V, James C, Trannoy S, Masse A, Kosmider O, Le Couedic JP, Robert F, Alberdi A, et al. Mutation in TET2 in myeloid cancers. The New England journal of medicine. 2009; 360:2289–2301. [PubMed: 19474426]

Figueroa ME, Abdel-Wahab O, Lu C, Ward PS, Patel J, Shih A, Li Y, Bhagwat N, Vasanthakumar A, Fernandez HF, et al. Leukemic IDH1 and IDH2 mutations result in a hypermethylation phenotype, disrupt TET2 function, and impair hematopoietic differentiation. Cancer Cell. 2010; 18:553–567. [PubMed: 21130701]

Genovese G, Kahler AK, Handsaker RE, Lindberg J, Rose SA, Bakhoum SF, Chambert K, Mick E, Neale BM, Fromer M, et al. Clonal Hematopoiesis and Blood-Cancer Risk Inferred from Blood DNA Sequence. N Engl J Med. 2014

Gilliland DG, Griffin JD. The roles of FLT3 in hematopoiesis and leukemia. Blood. 2002; 100:1532–1542. [PubMed: 12176867]

Goardon N, Marchi E, Atzberger A, Quek L, Schuh A, Soneji S, Woll P, Mead A, Alford KA, Rout R, et al. Coexistence of LMPP-like and GMP-like leukemia stem cells in acute myeloid leukemia. Cancer Cell. 2011; 19:138–152. [PubMed: 21251617]

Groschel S, Sanders MA, Hoogenboezem R, de Wit E, Bouwman BA, Erpelinck C, van der Velden VH, Havermans M, Avellino R, van Lom K, et al. A Single Oncogenic Enhancer Rearrangement Causes Concomitant EVI1 and GATA2 Deregulation in Leukemia. Cell. 2014; 157:369–381. [PubMed: 24703711]

Guo JU, Su Y, Zhong C, Ming GL, Song H. Hydroxylation of 5-methylcytosine by TET1 promotes active DNA demethylation in the adult brain. Cell. 2011; 145:423–434. [PubMed: 21496894]

Heuser M, Yun H, Berg T, Yung E, Argiropoulos B, Kuchenbauer F, Park G, Hamwi I, Palmqvist L, Lai CK, et al. Cell of origin in AML: susceptibility to MN1-induced transformation is regulated by the MEIS1/AbdB-like HOX protein complex. Cancer Cell. 2011; 20:39–52. [PubMed: 21741595]

Hou HA, Lin CC, Chou WC, Liu CY, Chen CY, Tang JL, Lai YJ, Tseng MH, Huang CF, Chiang YC, et al. Integration of cytogenetic and molecular alterations in risk stratification of 318 patients with de novo non-M3 acute myeloid leukemia. Leukemia. 2014; 28:50–58. [PubMed: 23929217]

Jaiswal S, Fontanillas P, Flannick J, Manning A, Grauman PV, Mar BG, Lindsley RC, Mermel CH, Burtt N, Chavez A, et al. Age-Related Clonal Hematopoiesis Associated with Adverse Outcomes. N Engl J Med. 2014

Jan M, Snyder TM, Corces-Zimmerman MR, Vyas P, Weissman IL, Quake SR, Majeti R. Clonal evolution of preleukemic hematopoietic stem cells precedes human acute myeloid leukemia. Science translational medicine. 2012; 4:149ra118.

Ji H, Ehrlich LI, Seita J, Murakami P, Doi A, Lindau P, Lee H, Aryee MJ, Irizarry RA, Kim K, et al. Comprehensive methylome map of lineage commitment from haematopoietic progenitors. Nature. 2010; 467:338–342. [PubMed: 20720541]

Kats LM, Reschke M, Taulli R, Pozdnyakova O, Burgess K, Bhargava P, Straley K, Karnik R, Meissner A, Small D, et al. Proto-Oncogenic Role of Mutant IDH2 in Leukemia Initiation and Maintenance. Cell Stem Cell. 2014; 14:329–341. [PubMed: 24440599]

Kayser S, Levis MJ. FLT3 tyrosine kinase inhibitors in acute myeloid leukemia: clinical implications and limitations. Leuk Lymphoma. 2014; 55:243–255. [PubMed: 23631653]

Kirstetter P, Schuster MB, Bereshchenko O, Moore S, Dvinge H, Kurz E, Theilgaard-Monch K, Mansson R, Pedersen TA, Pabst T, et al. Modeling of C/EBPalpha mutant acute myeloid leukemia reveals a common expression signature of committed myeloid leukemia-initiating cells. Cancer Cell. 2008; 13:299–310. [PubMed: 18394553]

Ko M, Huang Y, Jankowska AM, Pape UJ, Tahiliani M, Bandukwala HS, An J, Lamperti ED, Koh KP, Ganetzky R, et al. Impaired hydroxylation of 5-methylcytosine in myeloid cancers with mutant TET2. Nature. 2010; 468:839–843. [PubMed: 21057493]

Krivtsov AV, Twomey D, Feng Z, Stubbs MC, Wang Y, Faber J, Levine JE, Wang J, Hahn WC, Gilliland DG, et al. Transformation from committed progenitor to leukaemia stem cell initiated by MLL-AF9. Nature. 2006; 442:818–822. [PubMed: 16862118]

Langemeijer SM, Kuiper RP, Berends M, Knops R, Aslanyan MG, Massop M, Stevens-Linders E, van Hoogen P, van Kessel AG, Raymakers RA, et al. Acquired mutations in TET2 are common in myelodysplastic syndromes. Nat Genet. 2009; 41:838–842. [PubMed: 19483684]

Lee BH, Williams IR, Anastasiadou E, Boulton CL, Joseph SW, Amaral SM, Curley DP, Duclos N, Huntly BJ, Fabbro D, et al. FLT3 internal tandem duplication mutations induce myeloproliferative or lymphoid disease in a transgenic mouse model. Oncogene. 2005; 24:7882–7892. [PubMed: 16116483]

Li S, Garrett-Bakelman FE, Akalin A, Zumbo P, Levine R, To BL, Lewis ID, Brown AL, D'Andrea RJ, Melnick A, Mason CE. An optimized algorithm for detecting and annotating regional differential methylation. BMC Bioinformatics. 2013; 14(Suppl 5):S10. [PubMed: 23735126]

Li Z, Cai X, Cai CL, Wang J, Zhang W, Petersen BE, Yang FC, Xu M. Deletion of Tet2 in mice leads to dysregulated hematopoietic stem cells and subsequent development of myeloid malignancies. Blood. 2011; 118:4509–4518. [PubMed: 21803851]

Liberzon A, Subramanian A, Pinchback R, Thorvaldsdottir H, Tamayo P, Mesirov JP. Molecular signatures database (MSigDB) 3.0. Bioinformatics. 2011; 27:1739–1740. [PubMed: 21546393]

Madzo J, Liu H, Rodriguez A, Vasanthakumar A, Sundaravel S, Caces DB, Looney TJ, Zhang L, Lepore JB, Macrae T, et al. Hydroxymethylation at Gene Regulatory Regions Directs Stem/Early Progenitor Cell Commitment during Erythropoiesis. Cell Rep. 2014; 6:231–244. [PubMed: 24373966]

Metzeler KH, Maharry K, Radmacher MD, Mrozek K, Margeson D, Becker H, Curfman J, Holland KB, Schwind S, Whitman SP, et al. TET2 mutations improve the new European LeukemiaNet risk classification of acute myeloid leukemia: a Cancer and Leukemia Group B study. J Clin Oncol. 2011; 29:1373–1381. [PubMed: 21343549]

Moran-Crusio K, Reavie L, Shih A, Abdel-Wahab O, Ndiaye-Lobry D, Lobry C, Figueroa ME, Vasanthakumar A, Patel J, Zhao X, et al. Tet2 loss leads to increased hematopoietic stem cell self-renewal and myeloid transformation. Cancer Cell. 2011; 20:11–24. [PubMed: 21723200]

Patel JP, Gonen M, Figueroa ME, Fernandez H, Sun Z, Racevskis J, Van Vlierberghe P, Dolgalev I, Thomas S, Aminova O, et al. Prognostic relevance of integrated genetic profiling in acute myeloid leukemia. N Engl J Med. 2012; 366:1079–1089. [PubMed: 22417203]

Pronier E, Almire C, Mokrani H, Vasanthakumar A, Simon A, da Costa Reis Monte Mor B, Masse A, Le Couedic JP, Pendino F, Carbonne B, et al. Inhibition of TET2-mediated conversion of 5-methylcytosine to 5-hydroxymethylcytosine disturbs erythroid and granulomonocytic differentiation of human hematopoietic progenitors. Blood. 2011; 118:2551–2555. [PubMed: 21734233]

Quivoron C, Couronne L, Della Valle V, Lopez CK, Plo I, Wagner-Ballon O, Do Cruzeiro M, Delhommeau F, Arnulf B, Stern MH, et al. TET2 inactivation results in pleiotropic hematopoietic abnormalities in mouse and is a recurrent event during human lymphomagenesis. Cancer Cell. 2011; 20:25–38. [PubMed: 21723201]

Rampal R, Alkalin A, Madzo J, Vasanthakumar A, Pronier E, Patel J, Li Y, Ahn J, Abdel-Wahab O, Shih A, et al. DNA Hydroxymethylation Profiling Reveals that WT1 Mutations Result in Loss of TET2 Function in Acute Myeloid Leukemia. Cell Rep. 2014; 9:1841–1855. [PubMed: 25482556]

Rohle D, Popovici-Muller J, Palaskas N, Turcan S, Grommes C, Campos C, Tsoi J, Clark O, Oldrini B, Komisopoulou E, et al. An inhibitor of mutant IDH1 delays growth and promotes differentiation of glioma cells. Science. 2013; 340:626–630. [PubMed: 23558169]

Sarry JE, Murphy K, Perry R, Sanchez PV, Secreto A, Keefer C, Swider CR, Strzelecki AC, Cavelier C, Recher C, et al. Human acute myelogenous leukemia stem cells are rare and heterogeneous when assayed in NOD/SCID/IL2Rgammac-deficient mice. J Clin Invest. 2011; 121:384–395. [PubMed: 21157036]

Smith CC, Wang Q, Chin CS, Salerno S, Damon LE, Levis MJ, Perl AE, Travers KJ, Wang S, Hunt JP, et al. Validation of ITD mutations in FLT3 as a therapeutic target in human acute myeloid leukaemia. Nature. 2012; 485:260–263. [PubMed: 22504184]

Snow JW, Trowbridge JJ, Fujiwara T, Emambokus NE, Grass JA, Orkin SH, Bresnick EH. A single cis element maintains repression of the key developmental regulator Gata2. PLoS Genet. 2010; 6:e1001103. [PubMed: 20838598]

Tahiliani M, Koh KP, Shen Y, Pastor WA, Bandukwala H, Brudno Y, Agarwal S, Iyer LM, Liu DR, Aravind L, Rao A. Conversion of 5-methylcytosine to 5-hydroxymethylcytosine in mammalian DNA by MLL partner TET1. Science. 2009; 324:930–935. [PubMed: 19372391]

Traina F, Visconte V, Elson P, Tabarroki A, Jankowska AM, Hasrouni E, Sugimoto Y, Szpurka H, Makishima H, O'Keefe CL, et al. Impact of molecular mutations on treatment response to DNMT inhibitors in myelodysplasia and related neoplasms. Leukemia. 2014; 28:78–87. [PubMed: 24045501]

Wang F, Travins J, DeLaBarre B, Penard-Lacronique V, Schalm S, Hansen E, Straley K, Kernytsky A, Liu W, Gliser C, et al. Targeted inhibition of mutant IDH2 in leukemia cells induces cellular differentiation. Science. 2013; 340:622–626. [PubMed: 23558173]

Welch JS, Ley TJ, Link DC, Miller CA, Larson DE, Koboldt DC, Wartman LD, Lamprecht TL, Liu F, Xia J, et al. The origin and evolution of mutations in acute myeloid leukemia. Cell. 2012; 150:264–278. [PubMed: 22817890]

Wong DJ, Liu H, Ridky TW, Cassarino D, Segal E, Chang HY. Module map of stem cell genes guides creation of epithelial cancer stem cells. Cell Stem Cell. 2008; 2:333–344. [PubMed: 18397753]

Xie M, Lu C, Wang J, McLellan MD, Johnson KJ, Wendl MC, McMichael JF, Schmidt HK, Yellapantula V, Miller CA, et al. Age-related mutations associated with clonal hematopoietic expansion and malignancies. Nat Med. 2014; 20:1472–1478. [PubMed: 25326804]

Zuber J, Radtke I, Pardee TS, Zhao Z, Rappaport AR, Luo W, McCurrach ME, Yang MM, Dolan ME, Kogan SC, et al. Mouse models of human AML accurately predict chemotherapy response. Genes Dev. 2009; 23:877–889. [PubMed: 19339691]

Significance

Specific combinations of AML disease alleles confer adverse outcomes and define subtypes; however, in vivo models do not exist for the majority of common, poor-prognosis genotypes. Here we show that *TET2* and *FLT3* mutations cooperate to induce AML using a mouse model. This model has a defined leukemia stem cell population with a characteristic transcriptional and epigenetic profile and is critical for therapeutic targeting. The methylation changes exhibit cooperativity of disease alleles to target multiple loci. These data also suggest that leukemic transformation by these epigenetic changes is reversible, and therapies that reactivate silenced genes may improve outcomes for AML patients.

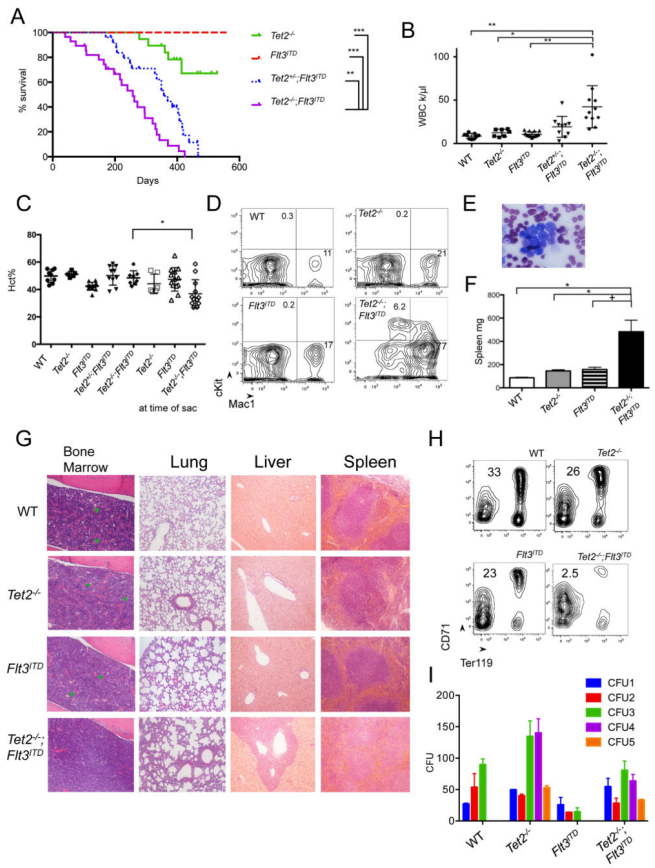

Figure 1. Development of leukemic disease in *VTet2$^{-/-}$Flt3^{ITD}*mice

(A) Kaplan Meir survival curve of *Tet2$^{-/-}$* (n=19), *Flt3^{ITD}* (n=23), *Tet2$^{+/-}$;Flt3^{ITD}* (n=26), and *Tet2$^{-/-}$;Flt3^{ITD}* (n=28). (B–D) Peripheral WBC count at 4 months (B), hematocrit at 4 months and at time of sacrifice (C), and peripheral blood Mac1 and cKit immunophenotype at 4 months (D), mean Mac1^{+} and cKit^{+} (n=5 to 12 per group). (E) Peripheral blood morphology in *Tet2$^{-/-}$;Flt3^{ITD}* mice. scale bar 10 µm. (F) Spleen weight at 4 months. (G) Histology of bone marrow, lung, liver and spleen of WT, *Tet2$^{-/-}$*, *Flt3^{ITD}*, *Tet2$^{-/-}$;Flt3^{ITD}* mice. Scale bar 100 µm bone marrow, lung, and liver; 200 µm spleen. Green arrowheads indicate megakaryocytes. (H) Bone marrow CD71 and Ter119 immunophenotype, gates mean (n=4 to 6 per genotype). (I) Serial plating in methylcellulose and colony counts (representative experiment of n=3). +p<=.05, *p<=.01, **p<=.001, ***p<=.0001. Survival statistics using long-rank test. Otherwise, p values using unpaired Student's t-test. Graphs mean±SEM. See also Figure S1.

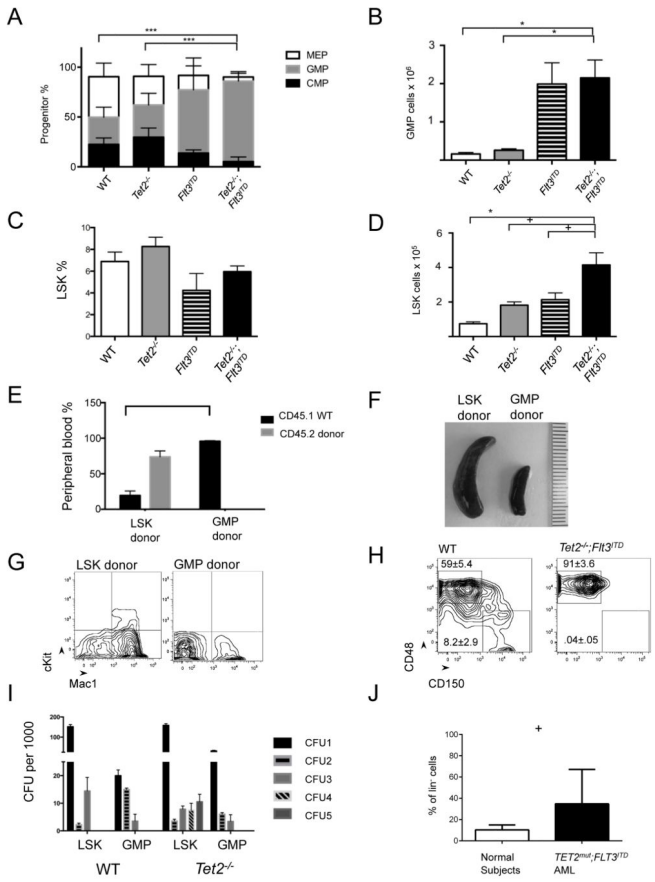

Figure 2. Stem-progenitor immunophenotype and transplantability of *VTet2*$^{-/-}$*Flt3*^{ITD}mice

(A,B) Relative frequency of CMP, GMP, and MEP progenitors in the lin^{-}Sca^{-}cKit^{+} cell fraction (A) and absolute GMP cell number (B) in bone marrow. (C,D) Relative frequency (C) and absolute cell number (D) of LSK cells in lin^{-} bone marrow (n=4 to 6). (E–G) Analysis of transplanted mice. Peripheral blood CD45.1 (host-derived marker) and CD45.2 (leukemia-derived marker) immunophenotype (E), representative spleen size (millimeter scale) (F), and representative peripheral blood Mac1 and cKit immunophenotype (G) of CD45.1^{+} recipient mice transplanted with CD45.2^{+} *Tet2*$^{-/-}$*;Flt3*^{ITD} LSK or GMP cells (n=4 per group). (H) Flow plot of bone marrow LSK cells for MPP (CD48^{+}CD150^{-}) and LT-HSC (CD48^{-}CD150^{+}) frequency in WT and *VTet2*$^{-/-}$*Flt3*^{ITD} mice, gate mean±SEM (n=4). (I) Re-plating colony counts of WT and *Tet2*$^{-/-}$ cells sorted for LSK and GMP populations (representative experiment from 3 replicates). (J) *TET2;FLT3*^{ITD} mutant human AML and normal subject ST-HSC/MPP frequency (n=9). +p<=.05, *p<=.01, ** p<=.001, ***p<=.0001. p values using unpaired Student's t-test. Graphs mean±SEM. See also Figure S2.

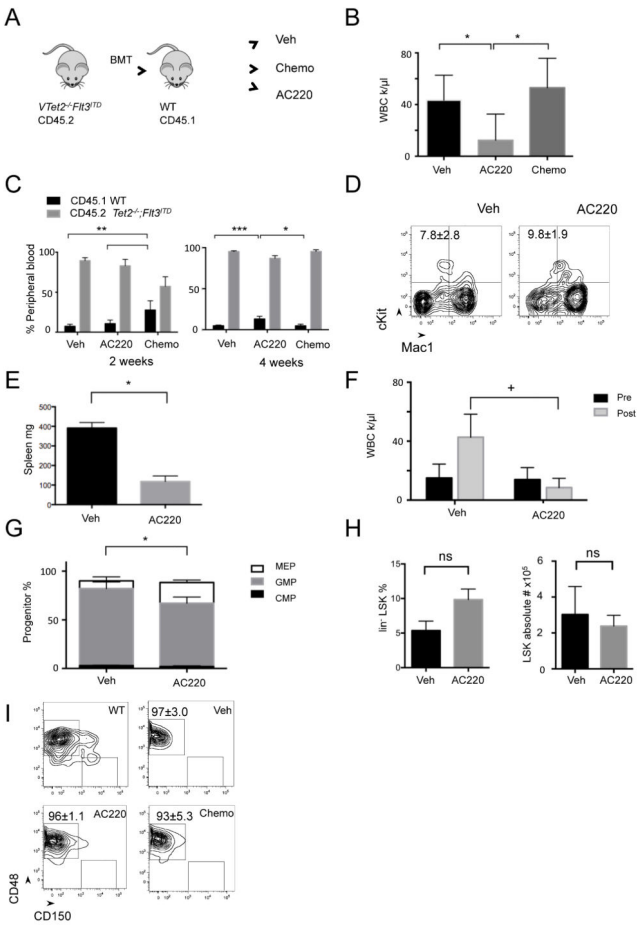

Figure 3. Response of *VTet2*$^{-/-}$*Flt3*^{ITD} leukemia to AC220 and chemotherapy

(A) Treatment scheme with secondary transplanted CD45.2^{+} *Tet2*$^{-/-}$*;Flt3*^{ITD} bone marrow into CD45.1^{+} mice (n=5 per group). (B–D) Peripheral blood WBC count after treatment for 4 weeks (B), CD45.1 (host-derived marker) and CD45.2 (leukemia-derived marker) immunophenotype at 2 weeks and 4 weeks (C), and Mac1 and cKit immunophenotype at 4 weeks (D) of vehicle, chemotherapy treated, and AC220 treated mice. (E,F) Spleen size (E) and peripheral blood WBC count (F) of *VTet2*$^{-/-}$*Flt3*^{ITD} mice treated with AC220 for 4 weeks (n=3 per group). (G–I) Bone marrow myeloid progenitor analysis (G), LSK percentage and absolute number (H), and SLAM LSK immunophenotype analysis, gates indicated for MPPs (CD48^{+}CD150^{-}) and LT-HSC (CD48^{-}CD150^{+}) fractions (I) following vehicle, chemotherapy, or AC220 treatment. +p<=.05, *p<=.01, **p<=.001, ***p<=.0001. p values using unpaired Student's t-test. Graphs and flow plot numbers, mean±SEM. See also Figure S3.

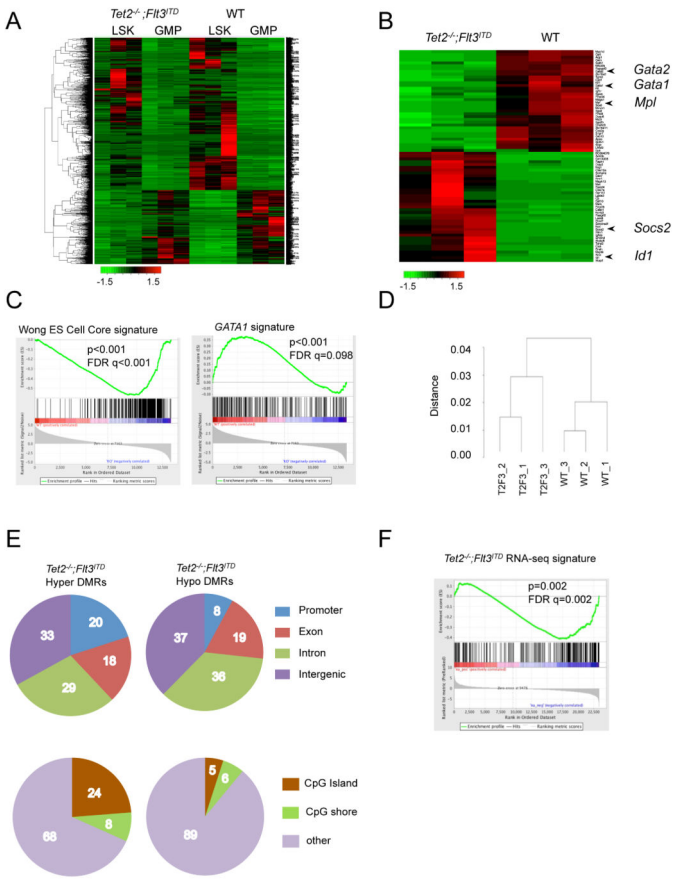

Figure 4. RNA-seq and methylation analysis of *VTet2$^{-/-}$Flt3^{ITD}* mice

(A,B) Heat map from RNA sequencing expression analysis of WT and *Tet2$^{-/-}$;Flt3^{ITD}* bone marrow LSK and GMP cells (A) and LSK cells for genes ranked by Fold Change >3.5 and FDR<10^{-5} (B). z-score scale. (C) GSEA enrichment plot of *Tet2$^{-/-}$;Flt3^{ITD}* LSK RNA expression correlated with the embryonic stem cell signature and negatively correlated with *GATA1* signature. (D) Dendrogram clustering based on eRRBS methylation profiles from WT and *Tet2$^{-/-}$;Flt3^{ITD}* (T2F3) LSK cells. (E) Gene localization of hypermethylated and hypomethylated differentially methylated regions (DMRs) in *Tet2$^{-/-}$;Flt3^{ITD}* LSK cells, percentages. (F) GSEA enrichment plot correlating hypermethylation promoter genes with genes with down-regulated expression trend in *Tet2$^{-/-}$;Flt3^{ITD}* LSK cells. See also Figure S4, Table S1–3.

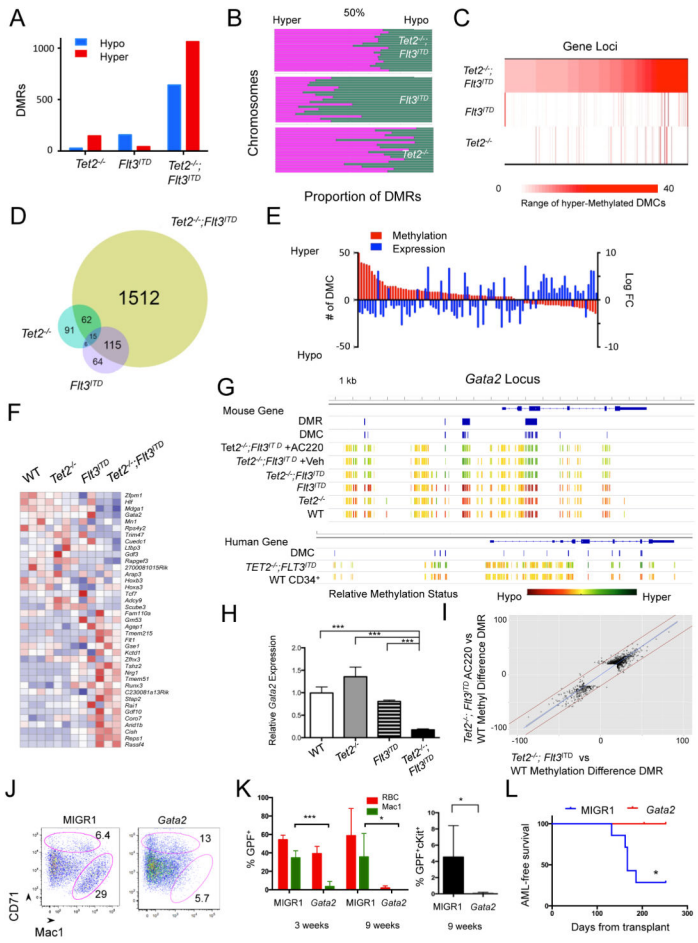

Figure 5. *Flt3*^{ITD} mutation and *Tet2* loss synergistically regulate gene expression

(A,B) Number of differentially methylated regions (DMRs) (A) and chromosomal hypermethylation and hypomethylation proportions (B) in *Tet2*$^{-/-}$, *Flt3*^{ITD}, *Tet2*$^{-/-}$;*Flt3*^{ITD} LSKs. (C) Heat map of number of hypermethylated differentially methylated cytosines (DMCs) in 424 genes in *Tet2*$^{-/-}$;*Flt3*^{ITD} LSKs compared to number of DMCs in *Tet2*$^{-/-}$ and *Flt3*^{ITD} LSKs. (D) Venn diagram of genes associated with DMRs for each genotype. (E) Bar graph of paired DMC number (in red) and expression change (in blue) for genes with promoter and intron DMCs and differential RNA expression. (F) Heat map of RNA expression based on genes in Table 1 (>=6 DMCs and altered expression in *Tet2*$^{-/-}$;*Flt3*^{ITD} LSKs) for LSKs of each genotype. z-score scale. (G) *Gata2* locus methylation for LSK cells, LSK cells following treatment, and human ST-HSC leukemia and CD34^{+} cell populations (scaled to average methylation). Also, location of DMRs and DMCs as determined through eRRBS analysis. (H) *Gata2* relative RNA expression in LSK cells. (I) Scatter plot of corresponding DMRs between *Tet2*$^{-/-}$;*Flt3*^{ITD} LSKs and *Tet2*$^{-/-}$;*Flt3*^{ITD} AC220 treated LSKs. Fitted line in blue; +/− 20% variation between samples by red lines. ($Pearson_{Corr}$=0.948) (J) CD71 and Mac1 immunophenotype of methylcellulose colonies from *Tet2*$^{-/-}$;*Flt3*^{ITD} cells expressing MIGR1 control or *Gata2*, mean gate frequency. (K,L) Peripheral blood GFP% of red blood cells (RBC), Mac1^{+} cells, and cKit^{+} cells at 3 weeks and 9 weeks (K) and leukemia free survival (L) of mice transplanted with MIGR1 (n=7) and

Gata2 (n=5) transduced *Tet2*$^{-/-}$;*Flt3*^{ITD} bone marrow. *p<=.01, ***p<.0001, using unpaired Student's t-test. Graphs mean±SEM. Survival statistic by long-rank test. See also Figure S5, Table S4 – S7.

Cancer Cell. Author manuscript; available in PMC 2016 April 13.

Table 1

Genes demonstrating synergistic interaction of $Tet2^{-/-}$ and $Flt3^{ITD}$ on methylation in $Tet2^{-/-}$;$Flt3^{ITD}$ LSK cells, with altered gene expression.

Gene Symbol	Hyper DMC number[a]			Hypo DMC number[a]			log2FC
	T2F3	$Tet2^{-/-}$	$Flt3^{ITD}$	*T2F3*	$Tet2^{-/-}$	$Flt3^{ITD}$	
MN1	91	3	0	0	0	0	−2.24
HOXA3	51	0	1	0	3	1	−2.19
GATA2	39	0	12	0	2	1	−2.99
ZFPM1	27	0	2	0	0	0	−2.85
GM53	23	0	0	0	0	1	6.92
LTBP3	22	0	0	0	0	0	−1.68
GSE1	23	0	4	2	2	0	−1.42
FAM110A	17	0	0	0	0	0	−1.26
RAPGEF3	15	0	4	0	0	0	−2.88
TRIM47	14	0	3	0	1	0	−3.54
RUNX3	14	0	0	1	0	1	−1.05
GDF10	12	0	1	0	0	0	9.23
ADCY9	12	0	0	0	0	0	−1.64
HOXB3	12	0	0	0	0	0	−2.11
RPS4Y2	12	0	0	0	0	0	−3.48
TSHZ2	14	0	3	3	0	3	6.64
FLT1	12	0	1	1	0	0	2.31
SCUBE3	11	0	0	0	1	0	−1.65
CUEDC1	10	0	1	0	3	2	−1.86
2700081O15RIK	10	0	0	0	0	0	−2.10
STAP2	15	0	1	7	0	0	6.04
KCTD1	8	0	1	0	2	1	−1.05
ZFHX3	8	0	3	0	0	0	−1.21
NRG1	8	0	0	0	0	0	5.67
PCDHGB6	8	0	0	0	0	0	−2.46
HLF	7	10	2	0	0	0	−2.74
AGAP1	8	0	2	1	0	0	−1.30

Gene Symbol	Hyper DMC number[a]			Hypo DMC number[a]			log2FC
	T2F3	*Tet2*$^{-/-}$	*Flt3*^{ITD}	*T2F3*	*Tet2*$^{-/-}$	*Flt3*^{ITD}	
ARAP3	7	0	2	0	0	0	−1.56
TCF7	7	0	0	0	0	2	−1.78
C230081A13RIK	7	0	0	0	0	0	−1.02
GDF3	7	0	0	0	0	0	−4.66
RAI1	7	0	0	0	0	0	−1.12
MDGA1	7	0	1	1	0	0	−3.13
TMEM215	6	0	0	0	0	1	2.35
CORO7	6	0	0	0	0	0	−0.93
ARID1B	6	0	0	1	0	0	−1.03
TMEM51	6	0	0	2	0	0	3.61
RASSF4	0	0	0	6	0	0	2.31
REPS1	0	0	0	7	0	4	1.39
CISH	0	0	0	18	1	4	2.81

LSK, (lin^{-}Sca^{+}cKit^{+}) cells; Hyper, Hypermethylation; Hypo, Hypomethylation; *T2F3*, *Tet2*$^{-/-}$;*Flt3*^{ITD} synergy component; log2FC, log 2 fold change of gene expression in *Tet2*$^{-/-}$;*Flt3*^{ITD} LSKs compared to wild-type LSKs.

[a]DMC contribution of the allele or allele combination to overall gene methylation (gene body and 5kb 5′ region) calculated by logistic regression analysis, filtered for >=6 DMC.